ACS chemical biology

ACS AUTHORCHOICE

Articles

Cite This: ACS Chem. Biol. 2020, 15, 360−368

An Immune-Stimulatory Helix−Loop−Helix Peptide: Selective Inhibition of CTLA-4−B7 Interaction

Tharanga M.R. Ramanayake Mudiyanselage,[†] Masataka Michigami,[‡] Zhengmao Ye,[‡] Atsuko Uyeda,[§] Norimitsu Inoue,[∥] Kikuya Sugiura,[†] Ikuo Fujii,*[,‡] and Daisuke Fujiwara*[,‡]

[†]Department of Veterinary Science, Graduate School of Life and Environmental Sciences, Osaka Prefecture University, 1-58 Rinku-oraikita, Izumisano, Osaka 598-8531, Japan

[‡]Department of Biological Science, Graduate School of Science, Osaka Prefecture University, 1-1 Gakuen-cho, Naka-ku, Sakai, Osaka 599-8531, Japan

[§]Department of Biotechnology, Graduate School of Engineering, Osaka University, 2-1 Yamadaoka, Suita, Osaka 565-0871, Japan

[∥]Department of Tumor Immunology, Osaka International Cancer Institute, 3-1-69 Otemae, Chuo-ku, Osaka-shi, Osaka 541-8567, Japan

Supporting Information

ABSTRACT: Molecular-targeting peptides and mini-proteins are promising alternatives to antibodies in a wide range of applications in bioscience and medicine. We have developed a helix−loop−helix (HLH) peptide as an alternative to antibodies to inhibit specific protein interactions. Cytotoxic T lymphocyte antigen-4 (CTLA-4) downregulates immune responses of cytotoxic T-cells by interaction with B7-1, a co-stimulatory molecule expressed on antigen presenting cells (APCs). To induce immune stimulatory activity, we used directed evolution methods to generate a HLH peptide that binds to CTLA-4, inhibiting the CTLA-4−B7-1 interaction and inducing immune stimulatory activity. Yeast-displayed libraries of HLH peptides were constructed and screened against CTLA-4 and identified the binding peptide Y-2, which exhibits a moderate affinity. The affinity of Y-2 was improved by *in vitro* affinity maturation to afford a stronger binder, ERY2-4. Peptide ERY2-4 specifically bound to CTLA-4 with a K_D of 196.8 ± 2.3 nM, comparable to the affinity of the CTLA-4−B7-1 interaction. Furthermore, ERY2-4 inhibited the CTLA-4−B7-1 interaction with an IC_{50} of 1.1 ± 0.03 μM and blocked the interaction between CTLA-4 and dendritic cells (DCs) presenting B7 on their surface. Importantly, ERY2-4 showed no cross-reactivity against CD28, suggesting it does not suppress T-cell activation. Finally, in a mixed lymphocyte reaction assay with DCs and T cells, ERY2-4 enhanced an allogeneic lymphocyte response. Since CTLA-4 is a critical immune checkpoint for restricting the cancer immune response, this inhibitory HLH peptide represents a new class of drug candidates for immunotherapy.

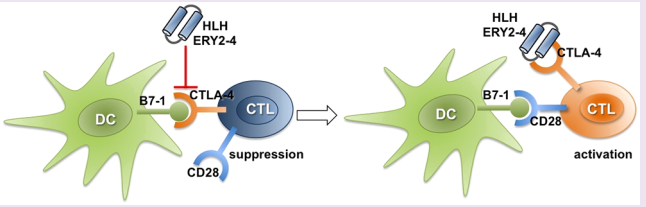

Antibodies are indisputably the most effective molecules for inhibiting protein−protein interactions (PPIs) in molecular targeting therapy. However, the use of antibodies has been limited due to their biophysical properties and high production cost, prompting extensive investigation of alternative binders for inhibiting PPIs to enable new applications.[1] Conformationally constrained polypeptides and mini-protein binders with high selectivity, efficacy, *in vivo* stability, and safety are promising alternatives to antibodies in a wide range of applications in bioscience and medicine.[2] For example, we have developed an alternative binding molecule, a helix−loop−helix (HLH) peptide, containing a nonimmunoglobulin domain.[3,4] This peptide is resistant to enzyme degradation *in vivo* and is too small to induce an immune response. We have constructed phage-display libraries of HLH peptides and obtained ligands and inhibitors for the granulocyte-colony stimulating factor receptor (G-CSFR), ganglioside GM1, and aurora kinase A.[5−7] Furthermore, an IgG-Fc-binding HLH peptide was designed using a protein grafting strategy.[3,8] Here, we describe the use of yeast surface-display libraries of HLH peptides to generate HLH peptide inhibitors for the cytotoxic T lymphocyte antigen-4 (CTLA-4)−B7-1 interaction occurring at immune checkpoints that suppress immune-stimulatory activity.

An immune checkpoint blockade enhances T cell activation against cancer cells.[9,10] Two signal pathways activate T cells: the antigenic-specific signal and the co-stimulatory signal. Both B7-1 and B7-2 are expressed on antigen presenting cells (APCs) and regulate co-stimulatory signals to T cells by binding to CD28 or CTLA-4 receptors on T cells.[11] T cell response is stimulated by CD28 and suppressed by CTLA-4. The inhibition of the T cell response by CTLA-4 is a critical inhibitory regulatory mechanism for T cell expansion.[9] Thus, inhibitors of the CTLA-4−B7-1 interaction could be used both

Received: September 18, 2019
Accepted: December 16, 2019
Published: December 16, 2019

DOI: 10.1021/acschembio.9b00743
ACS Chem. Biol. 2020, 15, 360−368

as research tools for chemical biology and as anticancer drugs. Anti-CTLA-4 monoclonal antibodies (mAbs) inhibited T regulatory (Treg) cell-mediated suppression of the antitumor immune response, resulting in the selective depletion of Treg cells in tumor lesions,[12] and increased cytokine production by activating T cells during antigenic stimulation in an *in vitro* cell proliferation system,[13] while anti-B7 antibodies suppress T cell activation.[14] The antibody drug ipilimumab binds to CTLA-4 and is effective against cancers by blocking the respective immune checkpoint,[9,10] thereby prolonging the overall survival of melanoma patients.[15] HLH peptide inhibitors targeting CTLA-4 are therefore successful alternatives to antibodies and hold promise as novel effective therapeutics against cancers.

In this work, we constructed yeast-displayed libraries of HLH peptides and screened them against Fc-fused human CTLA-4 (h-CTLA-4-Ig) using a combination of magnetic-activated cell sorting (MACS) and fluorescence-activated cell sorting (FACS). Peptide Y-2 was the most frequently sorted HLH peptide and showed specific binding to h-CTLA-4-Ig. Next, we examined the affinity maturation of peptide Y-2 using a secondary library constructed by error-prone PCR mutagenesis. The affinity-matured peptides ERY2-1, ERY2-4, and ERY2-6 exhibited strong affinities and high specificities for inhibiting the CTLA-4−B7 interaction. ERY2-4 showed a binding affinity comparable to that between CTLA-4 and B7 and inhibited the protein−protein interaction. Finally, mixed lymphocyte reaction (MLR) assay results showed that the addition of ERY2-4 increased allogeneic lymphocyte proliferation, suggesting that the blockade of the CTLA-4/B7 immune check-point enhances immune response.

RESULTS

Construction of Yeast Surface-Displayed Libraries of HLH Peptides. The generation of molecular-targeting HLH peptides is one approach to obtaining antibody alternatives for inhibiting PPIs.[3−8] The *de novo* designed HLH peptides consist of three regions: an N-terminal α-helix, a C-terminal α-helix, and a loop connecting the two helices (Figure 1a). We have constructed combinatorial HLH peptide libraries that retain the HLH structure. The conformationally constrained peptides reduce binding entropy, thus increasing binding affinity. In this study, HLH peptide libraries were constructed in which 12 amino acid residues in the helix regions were randomized and displayed on the surface of yeast, as described by Feldhaus et al. (Figure 1b).[16] The HLH peptides were linked to a FLAG tag and fused to the C-terminus of the yeast agglutinin protein Aga2p, which is attached to Aga1p on the yeast cell surface through disulfide bonds. The FLAG tag was used to detect the HLH peptides displayed on the yeast cell surface by using a combination of anti-FLAG mouse IgG and anti-mouse IgG antibody-Alexa 488. Two libraries, ΔPTA-12RC-1 (size: 3.2×10^8 variants) and ΔPTA-12RC-2 (size: 3.0×10^8 variants), were constructed using the yeast vector pYD11-BxXN (Figure S1).

Selection of Peptide Y-2 from HLH Peptide Libraries. A mixture of the yeast-displayed HLH peptide libraries ΔPTA-12RC-1 and ΔPTA-12RC-2 was screened against h-CTLA-4-Ig (abatacept), a fusion protein consisting of the extracellular domain of human CTLA-4 and the Fc domain of IgG_1 (Figure 2a). To allow screening by magnetic-activated cell sorting (MACS), h-CTLA-4-Ig was chemically modified with biotin to provide bio-h-CTLA-4-Ig, which then was bound to h-B7-1 with a binding activity comparable to that of nonlabeled h-

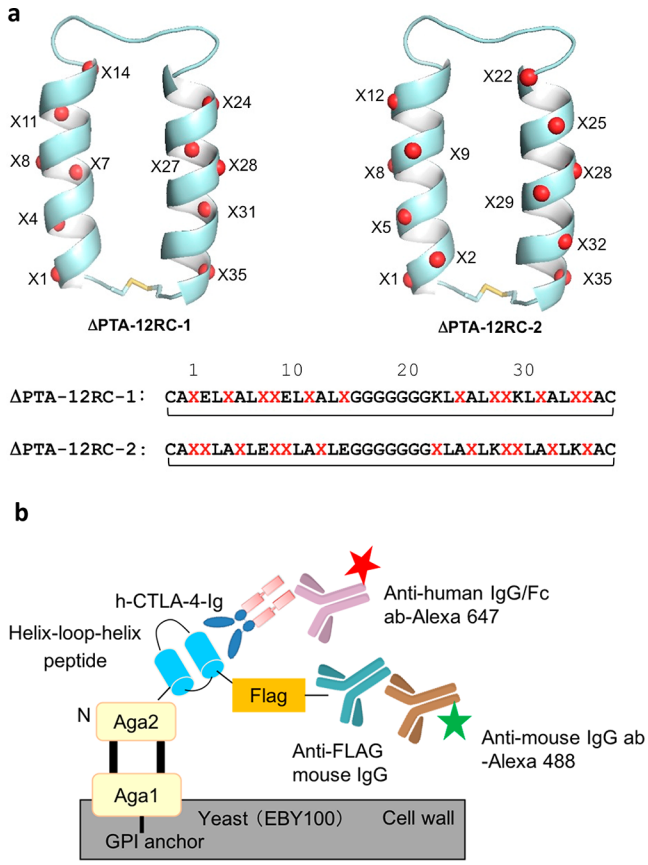

Figure 1. Yeast surface-displayed libraries of HLH peptides. (a) Each variable residue (X) in the libraries is encoded by an NDK degenerate codon that encodes 17 amino acids (C, D, E, F, G, H, I, K, L, M, N, Q, R, S, V, W, and Y). The sizes of the ΔPTA-12RC-1 and ΔPTA-12RC-2 libraries are 3.2×10^8 and 3.0×10^8 variants, respectively. (b) Schematic illustration of surface display on yeast. The HLH peptide was fused to the C-terminus of Aga2, followed by a FLAG tag.

CTLA-4-Ig (Figure S2). Streptavidin or antibiotin micro beads were alternately used during three rounds of MACS to remove nonspecific yeast clones. After these three rounds of screening against bio-CTLA-4-Ig, two rounds of FACS screening were conducted against nonlabeled h-CTLA-4-Ig using MACS-enriched bio-CTLA-4-Ig-binding clones, which were detected by anti-human IgG/Fc antibody-Alexa 647 (Figures 2a and S3). The enriched yeast cells within the P4 gate were sorted during the last round (Figure 2a). Fourteen individual yeast clones were randomly selected, and the amino acid sequences of the HLH peptides were deduced. Five different peptides were identified among the 14 sequences: Y-2, Y-4, Y-5, Y-6, and Y-11 (Table S1). Peptides Y-2, Y-5, and Y-6 were selected from the ΔPTA-12RC-2 library and peptides Y-4 and Y-11 were from the ΔPTA-12RC-1 library. The binding affinities of the yeast-displayed HLH peptides were determined by flow cytometry (FCM), with two-color fluorescence staining using streptavidin-APC and anti-FLAG-antibody-Alexa 488 (Figure 2b). All the yeast-displayed HLH peptides were bound to bio-h-CTLA-4-Ig in a dose-dependent manner, with Y-2 showing the highest affinity, with a K_D of 1.53 μM (Figure S4a). We therefore characterized peptide Y-2 in more detail.

FCM analysis indicated that yeast-displayed peptide Y-2 showed no binding activity to other biotinylated proteins (h-IgG-Fc, TNF-α, EGF, and BSA) and bound specifically to bio-

DOI: 10.1021/acschembio.9b00743
ACS Chem. Biol. 2020, 15, 360−368

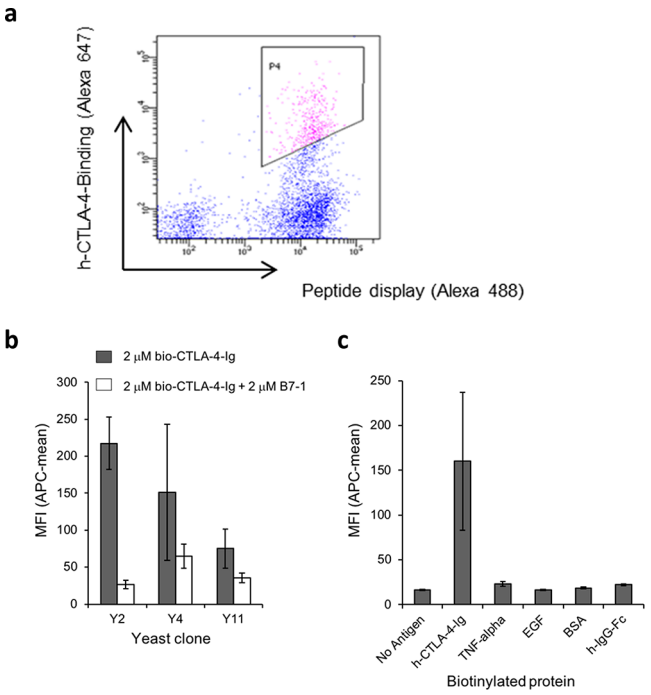

Figure 2. Identification and characterization of yeast-displayed HLH peptides binding to CTLA-4. (a) Dot plots of yeast clones from the final round of FACS screening in the presence of 10 μM h-CTLA-4-Ig. The yeast clones within the P4 gate were collected. (b) The FCM of the binding yeast clones Y-2, Y-4, and Y-11 for bio-h-CTLA-4-Ig (2.0 μM). The interactions were inhibited by h-B7-1-Fc (2.0 μM). (c) The FCM of clone Y-2 for bio-h-CTLA-4-Ig (2.0 μM) and other biotinylated proteins (2.0 μM).

h-CTLA-4-Ig (Figure 2c). This binding interaction was inhibited with 2.0 μM h-B7-1-Fc (Figure 2b). In addition, we produced a fusion protein (Trx-Y-2) comprising peptide Y-2 and thioredoxin (Trx) and used it to examine the binding affinity by ELISA. Human CTLA-4-Ig was immobilized on a plate and Trx-Y-2 was detected using an anti-thioredoxin antibody. Trx-Y-2 was bound to h-CTLA-4-Ig with a K_D of 1.97 μM, similar to that of yeast-displayed Y-2 (Figure S4b). Next, we improved the binding affinity of Y-2 by *in vitro* affinity maturation.

***In Vitro* Affinity Maturation of HLH Peptide Y-2.** Peptide Y-2 was randomly mutated to provide a secondary peptide library with 1×10^6 variants. Insert DNA fragments encoding the randomized peptides were prepared by error-prone PCR using the Y-2-encoding pET vector as a template and were inserted into the yeast display vector pYD11-BxXN. The yeast-displayed library was subjected to three rounds of MACS separation to enrich the yeast cells binding to bio-h-CTLA-4-Ig (Figure S5). Subsequent FACS with 100 nM h-CTLA-4-Ig resulted in a notable increase in binding clones (Figure S5). Finally, FACS screening with a low concentration (1.0 nM) of h-CTLA-4-Ig was conducted to sort the binding clones within gate P4 (Figure 3a). Ten yeast clones were randomly selected, and their amino acid sequences were deduced, resulting in the identification of three different peptides: ERY2-1, ERY2-4, and ERY2-6 with frequencies of 40, 50, and 10%, respectively, Figure 3b).

FCM analysis revealed that the yeast clones ERY2-1, ERY2-4, and ERY2-6 bound to bio-h-CTLA-4-Ig in a dose-dependent manner, with K_D values of 20.8 nM, 18.5 nM, and 20.7 nM, respectively (Figure 3c, S6). Thus, *in vitro* affinity maturation was successful in improving the binding affinity; the K_D values of the variants were 75-fold lower than that of the original yeast-displayed peptide. As shown in Figure 3c, the 100 nM h-B7-1-Fc completely inhibited the interactions of the yeast-displayed peptides and 10 nM bio-h-CTLA-4-Ig, suggesting that the peptides and h-B7-1 competitively bind to the same region on CTLA-4. These yeast-displayed peptides exhibited no binding activity to other biotinylated proteins (50 nM), including the TNF-α, EGF, h-IgG-Fc, BSA, and h-anti-B7-1 antibody, showing that their binding activity was specific to CTLA-4 (Figure 3d).

The immune-checkpoint molecules CTLA-4 and CD28 possess structurally similar recognition sites to bind the ligand B7-1.[17] The differences in their affinities serve to selectively regulate CD28 and CTLA-4 functions.[18,19] We confirmed that CTLA-4 has a higher binding activity to B7-1 than does CD28 (Figures 3e and S7). However, stimulating the immune responses of T-cells requires that the immune-checkpoint inhibitors specifically bind CTLA-4 to inhibit only the CTLA-4−B7-1 interaction without disrupting the CD28−B7-1 interaction. We thus examined the binding selectivity of peptide ERY2-4 for CTLA-4 and CD28. The ELISA assay results (Figure 3e) showed that peptide ERY2-4 has a significant affinity for CTLA-4 and no affinity for CD28. Thus, peptide ERY2-4 was expected to selectively inhibit only the CTLA-4−B7-1 interaction and exhibit T cell activation activity.

Synthesis and Characterization of the Selected Peptides. The peptides Y-2, ERY2-1, ERY2-4, and ERY2-6 were synthesized using standard Fmoc solid phase methods: the peptides were modified by N-terminal acetylation and C-terminal amidation. For disulfide bond formation, peptides cleaved from a resin were dissolved in 0.1 M NH_4HCO_3 (pH 8) and were stirred overnight at room temperature (RT). All of the peptides were then purified by RP-HPLC (Scheme S1).

The CD spectra of Y-2, ERY2-1, ERY2-4, and ERY2-6 exhibited double minima at 208 and 222 nm, which is similar to the parent peptide YT1-S, showing that they retained α-helical conformations in PBS at 20 °C (Figure 4a). We used surface plasmon resonance (SPR) to estimate that the binding affinities (K_D values) of peptides Y-2, ERY2-1, ERY2-4, and ERY2-6 for h-CTLA-4-Ig were 6.4 μM, 277.7 nM, 196.8 nM, and 571.7 nM, respectively (Figures 4b and S8, Table S2). The K_D value of B7-1 for h-CTLA-4-Ig was about 200 nM, as reported previously (Figure S2).[20] These observations suggested that ERY2-4 would have a comparable binding affinity for B7-1 and thus would be capable of inhibiting the CTLA-4−B7-1 interaction.

Inhibitory Activity of ERY2-4 against the Interaction between CTLA-4 and B7-1. SPR experiments revealed that peptides ERY2-1, ERY2-4, and ERY2-6 inhibited CTLA-4−B7-1 interaction, as shown in Figure 5a. In this assay, h-B7-1-Fc was immobilized on a sensor chip, and the IC_{50} values of the inhibitory activities of the peptides against the interaction between 270 nM h-CTLA-4-Ig and the immobilized h-B7-1-Fc were estimated. Peptides Y-2, ERY2-1, ERY2-4, and ERY2-6 showed IC_{50} values of 11.2, 0.92, 1.1, and 1.7 μM, respectively, while the control YT1-S showed no inhibitory activity.

Next, we examined a cell-based assay for the inhibitory activity of ERY2-4 against the CTLA-4−B7-1 interaction. Dendritic cells (DCs) expressing B7-1 were produced using monocytes from a human donor.[21,22] FCM analysis confirmed

DOI: 10.1021/acschembio.9b00743
ACS Chem. Biol. 2020, 15, 360−368

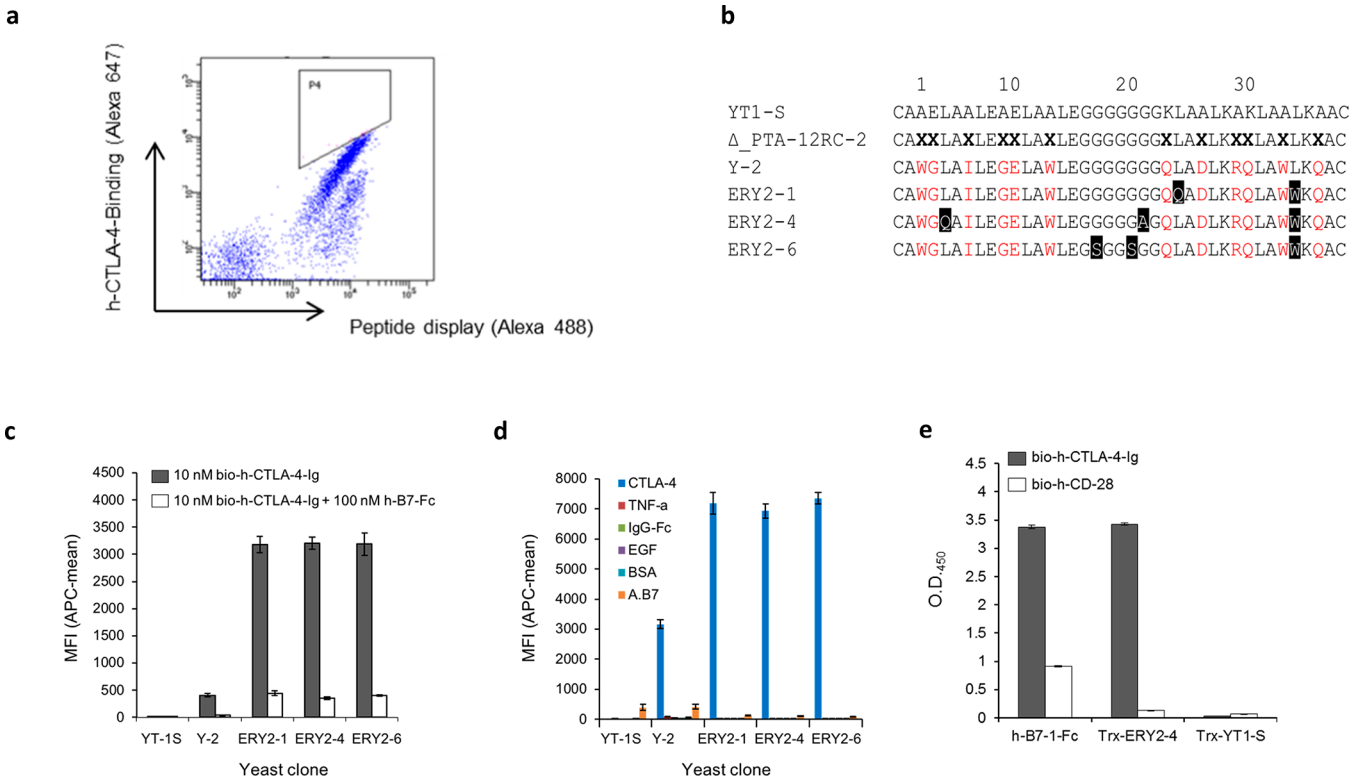

Figure 3. Affinity maturation of Y-2 and characterization of the isolated yeast clones. (a) Dot plots of the clones from the final round of FACS screening in the presence of 1 nM h-CTLA-4-Ig. The yeast clones within the P4 gate were collected. (b) Amino acid sequences of the HLH peptides. X represents a randomized amino acid. Selected residues from the libraries are shown in red and mutations are highlighted. (c) Interaction between 10 nM bio-h-CTLA-4-Ig and the isolated yeast clones and inhibition with 100 nM h-B7-1-Fc as analyzed by FCM. (d) Specificity of clones for 50 nM bio-h-CTLA-4-Ig. Peptide binding to 50 nM unrelated biotinylated proteins, including TNF-α, EGF, BSA, anti-B7-1, and h-IgG-Fc, was investigated by FCM analysis. (e) ELISA results showing the binding selectivity of peptide ERY2-4 for CTLA-4 and CD28. Thioredoxin-fused ERY2-4 (Trx-ERY2-4) was immobilized, and bound bio-h-CTLA-4-Ig and bio-h-CD28 were detected using a streptavidin-HRP conjugate. Human B7-1-Fc and thioredoxin-fused YT1-S (Trx-YT1-S) were used as controls.

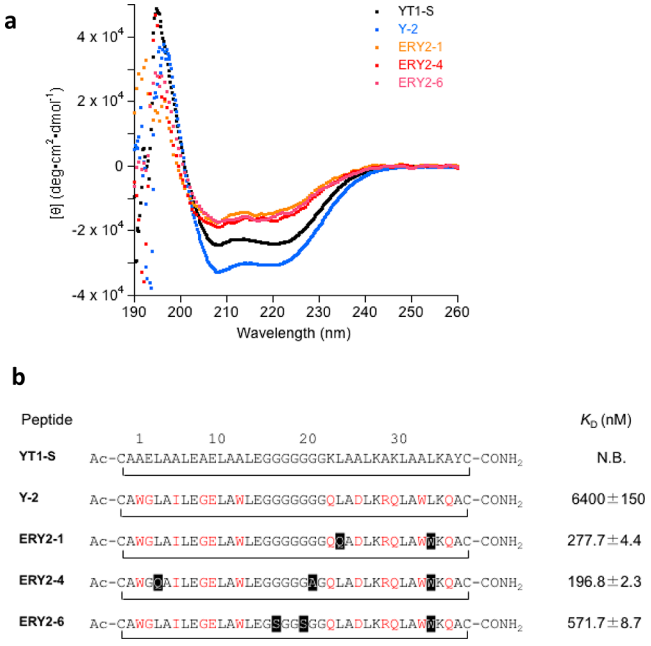

Figure 4. Structural characterization of the CTLA-4-binding peptides and their binding affinities. (a) CD spectra of the peptides recorded at 20 μM in PBS at 20 °C. (b) The HLH peptides were cyclized through a disulfide bond, and their K_D values were determined using SPR.

that h-CTLA-4-Ig bound to the DCs in a dose-dependent manner using anti-human IgG-Fc-FITC to detect bound h-CTLA-4-Ig (Figure S9). We also confirmed that the anti-CTLA-4 monoclonal antibody, a positive control, completely inhibited the interaction between 3 nM h-CTLA-4-Ig and B7-1 on the DCs (data not shown). Then, we investigated the inhibitory activity of ERY2-4 against the interaction between h-CTLA-4-Ig and B7 on DCs. Peptide ERY2-4 showed a dose-dependent inhibition, with an IC_{50} value of 631.9 ± 167.9 nM, while the control peptide YT1-S showed no inhibition (Figure 5b). Those observations suggested that ERY2-4 could induce a cancer immune response by functional blockade of CTLA-4.

Enhancement of Allogeneic Lymphocyte Responses by ERY2-4. An inhibitor exhibiting a functional blockade of CTLA-4 enhances allogeneic lymphocyte responses and thus demonstrates antitumor activity. We elucidated the biological activity of ERY2-4 using mixed lymphocyte reaction (MLR) assays (Figure 5c).[23] Prior to the cell-based assay, we confirmed the secondary structure of ERY2-4 at 37 °C and the stability (Tm = 57 °C) by CD spectroscopy as well as the binding activity (K_D = 298 nM) to h-CTLA-4-Ig at 37 °C by SPR (Figure S10, Table S2). A co-culture of allogeneic peripheral mononuclear cells and mature DCs was incubated with ERY2-4 or with YT1-S as a negative control at 37 °C. Mitotic cell division was detected by a thymidine incorporation assay. As expected, peptide ERY2-4 showed a 2-fold higher response compared to YT1-S, suggesting that the inhibition of

DOI: 10.1021/acschembio.9b00743
ACS Chem. Biol. 2020, 15, 360−368

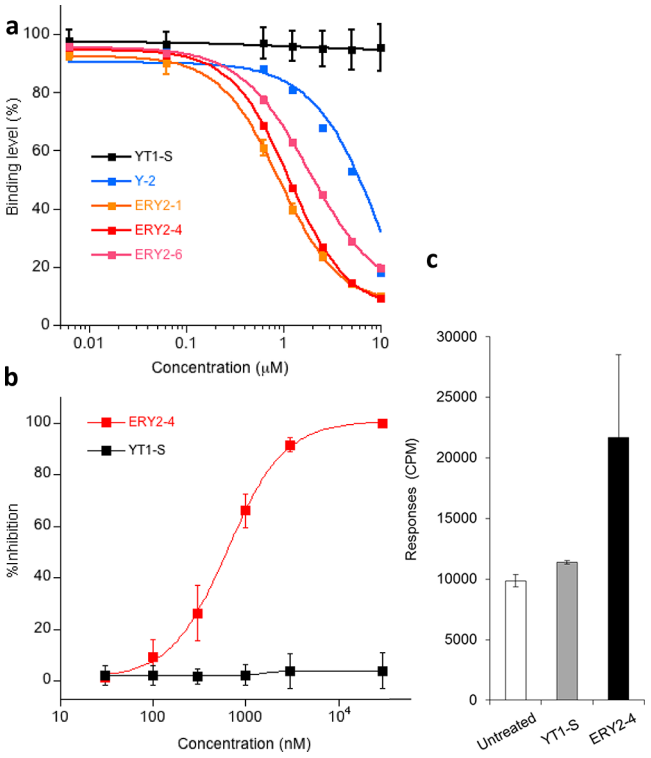

Figure 5. Inhibition of human CTLA-4−B7 interaction by Y-2 and ERY-2 peptides, leading to allogeneic lymphocyte stimulation activity. (a) IC_{50} curves for the HLH peptides against the interaction between h-CTLA-4-Ig and immobilized h-B7-1-Fc, as determined by SPR. (b) Blocking activity of ERY2-4 against the interaction between DCs-expressing B7 and h-CTLA-4-Ig, as estimated by FCM analysis. (c) Allogeneic lymphocyte proliferation in mixed lymphocyte cultures by peptide ERY2-4, as assayed using the thymidine incorporation assay.

the CTLA-4−B7-1 interaction by ERY2-4 regenerated the CD28−B7-1 interaction, inducing important co-stimulatory signals for T cell activation. Thus, peptide ERY2-4 is a potential alternative to antibodies as an immune checkpoint inhibitor in cancer therapy.

DISCUSSION

Here, we constructed the yeast-displayed HLH peptide libraries ΔPTA-12RC-1 and ΔPTA-12RC-2, in which 12 amino acids were randomized (Figure 1). We isolated yeast clones binding to h-CTAL-4-Ig by screening a mixture of the two libraries against h-CTLA-4-Ig (Figure 2a). Many (70%) of the clones were derived from ΔPTA-12RC-2, and 30% were derived from ΔPTA-12RC-1. Of the clones selected for further study, yeast-displayed Y-2 showed the highest binding activity to h-CTLA-4-Ig and also showed specific binding to h-CTLA-4-Ig (Figure 2c).

The sequence of peptide Y-2 was nonhomologous to the following CTLA-4 binders: the recognition site of B7,[18] the lipocalin-based binders,[24] the cystine-knot peptides,[25] and the paratopes of two FDA-approved therapeutic anti-CTLA-4 antibodies (tremelimumab and ipilimumab).[10,26] These binding domains form loop structures or nondefined secondary structures. In contrast, the binding domain of peptide Y-2 adopts an α-helical conformation (Figure 4a). CD spectra showed that the α-helical content of Y-2 was higher than that of the parent peptide YT1-S (Figure 4a). Asp27 and Arg30 of peptide Y-2 locate at i and i + 3 in the α-helix, forming a salt bridge to stabilize the α-helical structure.[27] We previously showed that the α-helical rigid structures of cyclized HLH peptides provide the proteolytic stability required for drug development.[3]

Synthetic peptide Y-2 bound to h-CTLA-4-Ig with a K_D value of 6.4 μM in SPR experiments (Figure 4b) and inhibited h-CTLA-4-Ig−B7-1 interaction with an IC_{50} value of 11.2 μM (Figure 5a). To obtain a more efficient inhibitor, we examined affinity maturation of peptide Y-2 using random mutagenesis, a commonly used method for the affinity maturation of peptides or protein ligands.[28] FACS screening under a strong selection pressure using 1.0 nM h-CTLA-4-Ig enriched the binding clones. FCM analyses provided K_D values for the yeast-displayed peptides ERY2-1, ERY2-4, and ERY2-6 of 20.8, 18.5, and 20.7 nM, respectively (Figures 3c and S6). On the other hand, the synthetic peptides ERY2-1, ERY2-4, and ERY2-6 showed K_D values of 278, 197, and 571 nM in SPR experiments, respectively (Figures 4b and S8, Table S2). This difference in K_D values between the yeast-displayed and synthetic peptides is due to an avidity effect.[29] In general, a yeast cell displays 10^4−10^5 copies of the gene-encoded polypeptide on the surface.[16] The polyvalent surface display probably magnified the apparent dissociation constants of the HLH peptides to h-CTLA-4-Ig.

A sequence comparison of the affinity-matured peptides ERY2-1, ERY2-4, and ERY2-6 showed the conserved mutation of L33W, suggesting that Trp33 is an additional epitope and increases the binding activities of the peptides to h-CTLA-4-Ig. On the other hand, the CD spectra revealed that the affinity-matured peptides had a lower α-helical content than the parent peptide Y-2 (Figure 4). Since Leu33 is an important residue for forming the intramolecular hydrophobic core that stabilizes the HLH structure,[4] the absence of Leu33 decreased the α-helical content of the HLH peptides.

The binding affinity of the synthetic peptide ERY2-4 to CTLA-4 was comparable to that of B7-1 (Figure S2),[20] and thus ERY2-4 inhibited the CTLA-4−B7-1 interaction. The ability of ERY2-4 to inhibit the CTLA-4−B7 interaction was confirmed by SPR and cell-based assays. SPR experiments (Figure 5a) showed that synthetic peptide ERY2-4 inhibited the interaction between h-CTLA-4-Ig and h-B7-1-Fc with an IC_{50} value of 1.1 μM in a dose dependent manner, and the FCM analysis confirmed that peptide ERY2-4 inhibits the interaction of dendritic cells (DCs) and h-CTLA-4-Ig (Figure 5b).

Cytotoxic T lymphocytes (CTLs) are activated after CD28 on CTLs binds with B7 on antigen presenting cells (APCs). CTLA-4 is expressed on CTLs after activation, replacing CD28 bound with B7, generating an immune checkpoint, and suppressing signals to terminate CTL activation.[9−11] Peptide ERY2-4 showed a binding selectivity favorable for immune-stimulants. Although CTLA-4 is structurally similar to CD28,[17] ERY2-4 showed binding to bio-h-CTLA-4-Ig but not to bio-CD28 by ELISA (Figure 3e). Thus, ERY2-4 apparently showed selective inhibition of the CTLA-4−B7 interaction to reactivate CTLs without interrupting the CD28−B7 interaction. Microscopic observation during the MLR experiments (Figure 5c)[30] revealed an increase in cell cluster formation by ERY2-4 (data not shown). The immune-stimulatory effects were measured using the thymidine incorporation assay (Figure 5c).

CTLA-4 is also expressed on Treg cells. However, in contrast to CTLs, Treg cells are not suppressed but rather

DOI: 10.1021/acschembio.9b00743
ACS Chem. Biol. 2020, 15, 360−368

activated by the signals from CTLA-4 after binding to B7.[31] Therefore, blocking the CTLA-4−B7 interaction using peptide ERY2-4 prevents this suppression and elicits the reactivation of CTLs by restoring the interaction between CD28 and B7. Moreover, our findings suggest that the blocking by ERY2-4 is likely to be more effective in cancer therapy following the activation of CTLs by cancer vaccination using APCs.[32]

Compared with antibody drugs, one advantage of HLH peptides is that the cancer immune response does not elicit antibody-dependent cellular toxicity (ADCC). Anti-CTLA-4 antibodies can be used in cancer therapy to block the CTLA-4−B7 interaction. Recently, however, it has been reported that ADCC results in these antibodies killing both CTLA-4 expressing Treg cells and CTLs temporally expressing CTLA-4.[33,34] This adverse effect is due to the Fc region, which can stimulate natural killer cells. ADCC to the CTLs may result in significant decreases in immune responses against cancer. In contrast, peptide ERY2-4 is expected to effectively enhance cancer immune responses by blocking CTLA-4 without depleting CTLs. We anticipate that ERY2-4 can be used as a therapeutic to block CTLA-4 due to its high inhibitory activity against the CTLA-4−B7-1 interaction without the drawback of ADCC.

The nonimmunogenic nature of HLH peptides enables their therapeutic application in all animal species,[4] in contrast to the immunogenicity of therapeutic monoclonal antibodies, which greatly limits their clinical use.[1] Yeast-displayed HLH peptide libraries would be a powerful tool for generating molecular-targeting peptides that inhibit PPIs and as molecular tools in chemical biology and therapeutics.

METHODS

Preparation of Yeast-Displayed HLH Peptide Libraries. A new plasmid for displaying HLH peptide libraries was constructed. A helix−loop−helix peptide with a FLAG tag epitope was fused to the C-terminus of Aga2 to allow the display of the HLH peptide on the extra-cellular surface of *Saccharomyces cerevisiae* EBY100. A double-stranded synthetic spacer was prepared using the two oligonucleotides Nhe-Mlu-U (5′-CTAGCTCCATGGGTGGTGAGCTCGCGGCCG-CCTCGAGTGATTACAAGGATGACGACGATAAGTGA-3′) and Nhe-Mlu-L (5′-CGCGTCACTTATCGTCGTCATCCTTGTAAT-CACTCGAGGCGGCCGCGAGCTCACCACCCATGGAG-3′). These sequences contain restriction sites for NheI, NcoI, NotI, XhoI, and MluI, as well as a FLAG tag. A spacer was inserted into the NheI and MluI sites of pYD1 (Invitrogen), and then, a 1.8 kb stuffer sequence was inserted into the NcoI and NotI restriction sites of the plasmid.

The yeast-displayed HLH peptide library was prepared by a transformation using homologous recombination in yeast. Insert fragments encoding the HLH peptide libraries were prepared by overlap-extension PCR to provide approximately 50 base pairs of homology to the pYD11-BxXN vector. The pYD-BxXN vector was then restricted using the NcoI and XhoI sites. Yeast cells were transformed with the linearized vector and PCR products by electroporation; then, the yeast cells were grown in SDCAA medium in a shaker at 30 °C overnight. The medium was changed to SG/RCAA at an absorbance of 0.5−1.0 at 600 nm to induce HLH peptide expression overnight at 20 °C.

Biotinylation of h-CTLA4-Ig. h-CTLA-4-Ig, 1 mg; Orencia, abatacept (Bristol−Myers Squibb), dissolved in 1 mL of PBS, was biotinylated using an EZ-Link Sulfo-NHS-Biotin kit (ThermoFisher Scientific) by mixing a 1:20 molar ratio of h-CTLA-4-Ig to Sulfo-NHS-Biotin and incubating for 30 min at RT. The biotinylated h-CTLA-4-Ig was then desalted using a Zeba Spin Desalting Column, 7K MWCO, 0.5 mL (Millipore, ThermoFisher Scientific). The concentration of bio-h-CTLA-4-Ig was calculated using the absorbance at 280 nm, and the binding affinity of bio-h-CTLA-4-Ig was shown to be comparable to that of h-CTLA-4-Ig using a Biacore T200 instrument (GE Healthcare) (Figure S2).

Screening of Yeast-Displayed HLH Peptide Libraries for CTLA-4. Three rounds of MACS separation followed by two rounds of FACS screening were performed for the initial screening against CTLA-4 using the ΔPTA-12RC-1 and ΔPTA-12RC-2 libraries and for further affinity maturation of the secondary Y-2-based peptide library. Yeast clones binding to h-CTLA-4-Ig were isolated.[35]

In the initial screening by MACS separation, a mixture of the ΔPTA-12RC-1 and ΔPTA-12RC-2 yeast display libraries was screened for bio-h-CTLA-4-Ig using MidiMACS separation (Miltenyi Biotec). The library mixture was incubated with bio-h-CTLA-4-Ig at concentrations of 10, 5, and 5 μM for rounds 1, 2, and 3, respectively, for 1 h at RT. The affinity maturation of Y-2 was conducted by screening the secondary Y-2-based peptide library using MidiMACS for bio-h-CTLA-4-Ig at 110, 55, and 55 nM in rounds 1, 2, and 3, respectively. MACS separation was achieved by incubating the yeast cells with MACS microbeads conjugated with an antibiotin antibody in rounds 1 and 3 and with beads conjugated with streptavidin in round 2. Unbound yeast cells were removed. and the magnetic beads with captured cells were separated using a MACS cell separation column. The eluted output yeast cells were amplified for the subsequent round of MACS separation. The collected yeast cells were cultured after each round of screening in SDCAA medium, and HLH peptide expression was induced in SGRCAA medium.

FACS screening initially involved sorting the yeast clones enriched by MACS separation using a FACSAria III (Beckton Dickinson). The ΔPTA-12RC-1 and ΔPTA-12RC-2 libraries were screened by incubating the enriched yeast cells with 1 μM h-CTLA-4-Ig in round 1 and 10 μM in round 2, together with monoclonal anti-FLAG mouse IgG (Sigma-Aldrich) at RT for 1 h. The cells were then stained for 30 min on ice with the secondary antibodies anti-human IgG/Fc ab-Alexa 647 (Jackson ImmunoResearch) for h-CTLA-4-Ig and anti-mouse-IgG ab-Alexa 488 (ThermoFisher Scientific) for anti-FLAG mouse IgG. The stained cells were washed and resuspended with PBS containing 5 mg mL^{-1} BSA and 2 mM EDTA buffer and then analyzed by FCM. The yeast cell population was gated on forward- and side-scatter channels to remove debris and doublet cells. Yeast cells in the double-positive quadrant were selected from the drawn gate and propagated for the next round of screening. The secondary Y-2-based peptide library was also screened using FACS, and the enriched yeast cells were incubated with 100 nM h-CTLA-4-Ig in round 1 and 1 nM in round 2 for sorting. After the final sorting, selected clones were sequenced.

Construction of a Y-2-Based Secondary Library Using Error Prone PCR. We introduced random mutations into Y-2 using the primers Y2TrxRev (5′-GCGCACCTGCCTCGAGGAACCGCCT-CCGGAGCCTCCACCGCA -3)′ and Y2TrxFor (5′- GACGA-CGACGACAAGGCCATGGCTGAATGC -3′) for error-prone PCR.[28] Several mutations on average were introduced into each peptide by repeating the procedure 4 times. Each time, the desired fragment around 200 bp long was purified using a QIAquick gel extraction kit (Qiagen). The fourth PCR product and pYD11-BxXN were separately digested with the restriction enzymes XhoI and NcoI. After separate gel extractions for the insert and vector, the products were ligated using Ligation high Ver.2 (Toyobo). EBY100 competent cells were transformed by electroporation using the purified plasmid variants. The transformed yeast cells were propagated in pYD medium, and the medium was changed to SDCAA for yeast cell growth at 30 °C overnight.

Yeast-Displayed HLH Peptides and Their Binding Activities for CTLA-4. Yeast displaying Y-2; the affinity-matured peptides ERY2-1, ERY2-4, and ERY2-6; and the negative control YT1-S were grown in SDCAA, and peptide expression was induced in SGRCAA. The K_D values of the peptides were estimated by incubating each clone with serially diluted bio-h-CTLA-Ig (0, 1.5, 3, 6, 12.5, 25, 50, 100, and 200 nM) together with monoclonal anti-FLAG mouse IgG at RT for 30 min. The cells were stained with streptavidin-APC (ThermoFisher Scientific) and anti-mouse IgG ab-Alexa 488 on ice

DOI: 10.1021/acschembio.9b00743
ACS Chem. Biol. 2020, 15, 360−368

for 30 min. Dissociation constants were estimated by nonlinear regression curve-fitting of the mean fluorescence intensities (MFI) of streptavidin-APC (Figure S6). We investigated the binding specificities of the peptides to CTLA-4 using 50 nM bio-h-CTLA-Ig or the biotinylated proteins h-IgG-Fc, EGF, TNF-α, BSA, and anti-B7-1 antibody (Figure 3d). The HLH peptide binding site to CTLA-4 was investigated by preincubating the yeast clones with 10 nM bio-h-CTLA-4-Ig and 100 nM human B7-1-Fc (PeproTech) as a competitor and then stained as described above (Figure 3c).

Peptide Synthesis. HLH peptides were synthesized by standard Fmoc solid-phase methods and purified by reversed-phase high-performance liquid chromatography (RP-HPLC). The peptides were dissolved in 0.1 M NH_4HCO_3(pH 8) and stirred overnight at RT to cyclize through an intramolecular disulfide bond. The cyclized peptides were purified by RP-HPLC (Hitachi) with a C18 column with a 250 mm × 10 mm inside diameter (I.D.) (YMC) using a linear gradient of water containing 0.1% TFA and acetonitrile at a flow rate of 3 mL min^{-1} and were monitored at 280 nm. The disulfide bond formation reactions were monitored by RP-HPLC, MALDI-TOF MS, and the Ellman's test. The purified peptides were identified by matrix-assisted laser desorption ionization time-of-flight mass spectrometry (MALDI-TOF-MS) (Autoflex II, Bruker Daltonics) using α-cyano-4-hydroxy cinnamic acid (CCA) in acetonitrile/0.1% (v/v) TFA (1:2) as a matrix. Peptide purities were determined by analytical HPLC with a C18 column with a 250 mm × 4.6 mm I.D. (YMC) and were monitored at 220 nm. The purities were greater than 90%. The purified peptides were identified using MALDI-TOF MS (m/z). $[M + H]^+$, Calcd for Y-2: 4079.1, found 4077.7. $[M + H]^+$, Calcd for ERY2-1: 4167.1, found 4168.1. $[M + H]^+$, Calcd for ERY2-4: 4181.1, found 4181.4. $[M + H]^+$, Calcd for ERY2-6: 4212.1, found 4213.5.

Determination of the Affinities and Inhibitory Activities of the Peptides Using SPR. SPR measurements were carried out with a Biacore T200 instrument. In direct binding experiments, h-CTLA-4-Ig was immobilized on a CM5 sensor chip by a standard amine coupling method (2200 RUs) and blocked with ethanolamine. A reference cell was also blocked with ethanolamine. Binding activities were measured in HBS-EP$^+$ at 25 °C, and the K_D values were determined by analyzing the binding level at steady state. The inhibitory activities of the HLH peptides for the CTLA-4−B7-1 interaction were estimated using an inhibition assay. Human B7-1-Fc was immobilized on a CM5 sensor chip using a standard amine coupling method (108 RUs) and blocked with ethanolamine. A reference cell was also blocked with ethanolamine. Various concentrations of peptides were incubated with 270 nM h-CTLA-4-Ig in HBS-EP$^+$ at 25 °C, and the IC_{50} values were estimated.

Circular Dichroism (CD). The peptide concentrations were determined by measuring the absorbance of the aromatic residues. CD spectra were recorded in PBS at a peptide concentration of 20 μM on a J-820 spectrometer (Jasco) at 20 °C. Spectra were collected from 260 to 190 nm every 0.2 nm.

Recombinant Protein Production. YT1-S, Y-2, and ERY2-4 were cloned into pET-32a(+) (Novagen,) and transformed in BL21-Codon Plus (DE3)-RP cells. The transformed cells were grown in 50 mL of LB medium at 37 °C to an OD_{600} of 0.6 and induced with 0.5 mM IPTG at 20 °C overnight in a shaker. The cells were lysed in chilled binding buffer (50 mM Tris buffer, pH 7.4, 500 mM NaCl, 20 mM imidazole) and then centrifuged at 20380 × g for 20 min at 4 °C. The supernatant was filtered and incubated with 1 mL of nickel Sepharose beads (GE Healthcare), followed by elution using elution buffer (20 mM Tris buffer, pH 7.4, 500 mM NaCl, 500 mM imidazole). The eluted Trx-Y-2 was dialyzed in PBS at 4 °C overnight, which was concentrated using an Amicon Ultra (MWCO 10 kDa) (Millipore), and the purity was determined by SDS-PAGE.

Generation and Maturation of Monocyte-Derived DCs. Ethical clearance for this study was obtained from the Research Ethics Committee of the Graduate School of Life and Environmental Sciences and the Graduate School of Science, Osaka Prefecture University. Mature DCs were generated from peripheral blood monocytes as described by Piemonti et al.[21] Peripheral blood (PB) was collected from a healthy human donor, and the buffy coat was separated by density centrifugation using a lymphocyte separation solution (Nacalai Tesque). PB mononuclear cells (PBMCs) were obtained from the buffy coat. CD14$^+$ peripheral blood monocytes (PBMOs) were isolated from the PBMCs using MACS by incubating with anti-human CD14 microbeads (Miltenyi Biotec). Differentiation of the monocytes into mature DCs was induced by suspending the cells in RPMI 1640 at a density of 1 × 10^6 cells mL^{-1}. The medium was supplemented with 10% FBS, 50 ng mL^{-1} human GM-CSF (PeproTech), and 10 ng mL^{-1} IL-4 (PeproTech). The cells were cultured for 5 days at 37 °C under 5% CO_2 in air, and then, half the medium was replaced with fresh medium containing cytokines on day 4. The cells were matured by incubating with 50 μg mL^{-1} PolyI:C (Sigma-Aldrich) for 48 h.[22] Matured DCs were labeled with anti-CD83-FITC (ThermoFisher Scientific) and anti-CD40-Alexa 647 antibodies (Bio-Rad) to detect the expression levels of CD83 and CD40, respectively, by FCM. 96% of mature DCs expressed both CD83 and CD40.

FCM Competition Assay. A serial dilution of ERY2-4, YT1-S (as a negative control), or human anti-CTLA-4 monoclonal antibody (ThermoFisher Scientific) (as a positive control) was mixed with 3 nM h-CTLA-4-Ig and added to 1.0 × 10^5 matured DCs. The samples were incubated at RT for 30 min, washed, and stained using goat anti-human IgG-Fc-FITC (Jackson Immuno Research) for h-CTLA-4-Ig and anti-CD40-Alexa 647 (eBioscience) for CD40 expressed on matured DCs. After incubation on ice for 30 min, DCs-bound h-CTLA-4-Ig was analyzed using a Bio-Rad S3 cell sorter (Bio-Rad). DCs-bound h-CTLA-4-Ig was quantified as the MFI values of goat anti-human IgG-Fc-FITC. Inhibition by ERY2-4 was quantified as the % inhibition, calculated by the following equation: [1 − (test MFI − positive control MFI)/(negative control MFI − positive control MFI) × 100%].[36] An IC_{50} value of ERY2-4 was derived from the nonlinear regression model for a dose-dependent increase of the % inhibition.

Mixed Lymphocyte Reaction (MLR) Assay. PBMCs were obtained by density centrifugation using a lymphocyte separation solution and were passed through a nylon wool column to enrich the lymphocytes, as described by Julius et al.[37] Additionally, the resultant cells were labeled with anti-CD3-PE (Invitrogen), anti-CD19-APC (Invitrogen), and anti-CD11b-FITC (ThermoFisher Scientific) antibodies, and the expression levels of CD3 (T cell), CD19 (B cell), and CD11b (monocyte) markers were detected by FCM to identify the percentages of T cells, B cells, and monocytes, respectively.[38] 62.5% of the enriched cells were T lymphocytes. The resultant cells (2 × 10^5 cells) were co-cultured with matured DCs (2 × 10^4 cells) in the presence of 30 μM ERY2-4, 30 μM YT1-S, or in the absence of peptide in round-bottom 96-well culture plates in triplicate for 4 days. The cultures were supplemented with 18.5 kBq of [^{3}H]-thymidine (PerkinElmer) and incubated for another 16 h. The cell cultures were harvested onto glass fiber filters, and the proliferative responses were evaluated by measuring the radioactivity of [^{3}H]-thymidine incorporated into the cellular DNA using a scintillation counter (Hitachi Healthcare Systems). The responses were expressed as counts per minute (CPM).

■ ASSOCIATED CONTENT

Supporting Information

The Supporting Information is available free of charge at https://pubs.acs.org/doi/10.1021/acschembio.9b00743.

Details of the experimental methods, supplementary Figures S1−S10, Scheme S1, and Tables S1 and S2 (PDF)

■ AUTHOR INFORMATION

Corresponding Authors

*E-mail: fujiwara@b.s.osakafu-u.ac.jp (D.F.).
*E-mail: fujii@b.s.osakafu-u.ac.jp (I.F.).

ORCID

Daisuke Fujiwara: 0000-0002-6230-5534

DOI: 10.1021/acschembio.9b00743
ACS Chem. Biol. 2020, 15, 360−368

Notes

The authors declare no competing financial interest.

■ ACKNOWLEDGMENTS

This research was partially supported by the Platform Project for Supporting Drug Discovery and Life Science Research (Basis for Supporting Innovative Drug Discovery and Life Science Research (BINDS)) from AMED under Grant Number 19am0101097j0003 and a Grant-in-Aid for Scientific Research (B) on the innovative area "Integrative animal science" (Project Number 16H05044) from the Japan Society for the Promotion of Science.

■ REFERENCES

(1) Binz, H. K., Amstutz, P., and Plückthun, A. (2005) Engineering novel binding proteins from nonimmunoglobulin domains. *Nat. Biotechnol. 23*, 1257−1268.

(2) Fosgerau, K., and Hoffmann, T. (2015) Peptide therapeutics: current status and future directions. *Drug Discovery Today 20*, 122−128.

(3) Fujiwara, D., Kitada, H., Oguri, M., Nishihara, T., Michigami, M., Shiraishi, K., Yuba, E., Nakase, I., Im, H., Cho, S., Joung, J. Y., Kodama, S., Kono, K., Ham, S., and Fujii, I. (2016) A Cyclized Helix - Loop - Helix Peptide as a Molecular Scaffold for the Design of Inhibitors of Intracellular Protein−Protein Interactions by Epitope and Arginine Grafting. *Angew. Chem., Int. Ed. 55*, 10612−10615.

(4) Suzuki, N., and Fujii, I. (1999) Optimazation of the loop length for folding of a helix-loop-helix. *Tetrahedron Lett. 40*, 6013−6017.

(5) El-Haggar, R., Kamikawa, K., Machi, K., Ye, Z., Ishino, Y., Tsumuraya, T., and Fujii, I. (2010) Molecular design of small organic molecules based on structural information for a conformationally constrained peptide that binds to G-CSF receptor. *Bioorg. Med. Chem. Lett. 20*, 1169−1172.

(6) Matsubara, T., Iida, M., Tsumuraya, T., Fujii, I., and Sato, T. (2008) Selection of a carbohydrate-binding domain with a helix-loop-helix structure. *Biochemistry 47*, 6745−6751.

(7) Fujiwara, D., Ye, Z., Gouda, M., Yokota, K., Tsumuraya, T., and Fujii, I. (2010) Selection of inhibitory peptides for Aurora-A kinase from a phage-displayed library of helix-loop-helix peptides. *Bioorg. Med. Chem. Lett. 20*, 1776−1778.

(8) Kawabata, K., Nagai, H., Konishi, N., Fujiwara, D., Sasaki, R., Ichikawa, T., and Fujii, I. (2014) Peptide-based immunoadsorbents: Molecular grafting of IgG−Fc-binding epitopes of Protein A onto a de novo-designed helix-loop-helix peptide. *Bioorg. Med. Chem. 22*, 1845−1849.

(9) Hendriks, L., and Besse, B. (2018) New windows open for immunotherapy in lung cancer. *Nature 558*, 376−377.

(10) Ramagopal, U. A., Liu, W., Garrett-Thomson, S. C., Bonanno, J. B., Yan, Q., Srinivasan, M., Wong, S. C., Bell, A., Mankikar, S., Rangan, V. S., Deshpande, S., Korman, A. J., and Almo, S. C. (2017) Structural basis for cancer immunotherapy by the first-in-class checkpoint inhibitor ipilimumab. *Proc. Natl. Acad. Sci. U. S. A. 114*, E4223−E4232.

(11) Greenfield, E. A., Nguyen, K. A., and Kuchroo, V. K. (1998) CD28/B7 costimulation: a review. *Crit. Rev. Immunol. 18*, 389−418.

(12) Simpson, T. R., Li, F., Montalvo-Ortiz, W., Sepulveda, M. A., Bergerhoff, K., Arce, F., Roddie, C., Henry, J. Y., Yagita, H., Wolchok, J. D., Peggs, K. S., Ravetch, J. V., Allison, J. P., and Quezada, S. A. (2013) Fc-dependent depletion of tumor-infiltrating regulatory T cells codefines the efficacy of anti-CTLA-4 therapy against melanoma. *J. Exp. Med. 210*, 1695−1710.

(13) Alegre, M. L., Shiels, H., Thompson, C. B., and Gajewski, T. F. (1998) Expression and Function of CTLA-4 in Th1 and Th2 cells. *J. Immunol. 161*, 3347−3356.

(14) Gribben, J. G., Guinan, E. V., Boussiotis, V. A., Ke, X. Y., Linsley, L., Sieff, C., Gray, G. S., Freeman, G. J., and Nadler, L. M. (1996) Complete blockade of B7 family-mediated costimulation is necessary to induce human alloantigen-specific anergy: a method to ameliorate graft-versus-host disease and extend the donor pool. *Blood 87*, 4887−4893.

(15) Snyder, A., Makarov, V., Merghoub, T., Yuan, J., Zaretsky, J. M., Desrichard, A., Walsh, L. A., Postow, M. A., Wong, P., Ho, T. S., Hollmann, T. J., Bruggeman, C., Kannan, K., Li, Y., Elipenahli, C., Liu, C., Harbison, C. T., Wang, L., Ribas, A., Wolchok, J. D., and Chan, T. A. (2014) Genetic Basis for Clinical Response to CTLA-4 Blockade in Melanom. *N. Engl. J. Med. 371*, 2189−2199.

(16) Feldhaus, M. J., Siegel, R. W., Opresko, L. K., Coleman, J. R., Feldhaus, J. M., Yeung, Y. A., Cochran, J. R., Heinzelman, P., Colby, D., Swers, J., Graff, C., Wiley, H. S., and Wittrup, K. D. (2003) Flow-cytometric isolation of human antibodies from a nonimmune Saccharomyces cerevisiae surface display library. *Nat. Biotechnol. 21*, 163−170.

(17) Harper, K., Balzano, C., Rouvier, E., Mattéi, M. G., Luciani, M. F., and Golstein, P. (1991) CTLA-4 and CD28 activated lymphocyte molecules are closely related in both mouse and human as to sequence, message expression, gene structure, and chromosomal location. *J. Immunol. 147*, 1037−44.

(18) Stamper, C. C., Zhang, Y., Tobin, J. F., Erbe, D. V., Ikemizu, S., Davis, S. J., Stahl, M. L., Seehra, J., Somers, W. S., and Mosyak, L. (2001) Crystal structure of the B7−1/CTLA-4 complex that inhibits human immune responses. *Nature 410*, 608−611.

(19) Collins, A. V., Brodie, D. W., Gilbert, R. J., Iaboni, A., Manso-Sancho, R., Walse, B., Stuart, D. I., van der Merwe, P. A., and Davis, S. J. (2002) The interaction properties of costimulatory molecules revisited. *Immunity 17*, 201−210.

(20) van der Merwe, P. A., Bodian, D. L., Daenke, S., Linsley, P., and Davis, S. J. (1997) CD80 (B7−1) binds both CD28 and CTLA-4 with a low affinity and very fast kinetics. *J. Exp. Med. 185*, 393−403.

(21) Piemonti, L., Monti, P., Allavena, P., Sironi, M., Soldini, L., Leone, B. E., Socci, C., and Di Carlo, V. (1999) Glucocorticoids affect human dendritic cell differentiation and maturation. *J. Immunol. 162*, 6473−6481.

(22) Navabi, H., Jasani, B., Reece, A., Clayton, A., Tabi, Z., Donninger, C., Mason, M., and Adams, M. (2009) A clinical grade poly I:C-analogue (Ampligen) promotes optimal DC maturation and Th1-type T cell responses of healthy donors and cancer patients in vitro. *Vaccine 27*, 107−115.

(23) Brown, J. A., Dorfman, D. M., Ma, F.-R., Sullivan, E. L., Munoz, O., Wood, C. R., Greenfield, E. A., and Freeman, G. J. (2003) Blockade of programmed death-1 ligands on dendritic cells enhances T cell activation and cytokine production. *J. Immunol. 170*, 1257−1266.

(24) Schönfeld, D., Matschiner, G., Chatwell, L., Trentmann, S., Gille, H., Hülsmeyer, M., Brown, N., Kaye, P. M., Schlehuber, S., Hohlbaum, A. M., and Skerra, A. (2009) An engineered lipocalin specific for CTLA-4 reveals a combining site with structural and conforma-tional features similar to antibodies. *Proc. Natl. Acad. Sci. U. S. A. 106*, 8198−8203.

(25) Maaß, F., Wüstehube-Lausch, J., Dickgießer, S., Valldorf, B., Reinwarth, M., Schmoldt, H. U., Daneschdar, M., Avrutina, O., Sahin, U., and Kolmar, H. (2015) Cystine-knot peptides targeting cancer-relevant human cytotoxic T lymphocyte-associated antigen 4 (CTLA-4). *J. Pept. Sci. 21*, 651−660.

(26) Lee, J. Y., Lee, H. T., Shin, W., Chae, J., Choi, J., Kim, S. H., Lim, H., Won Heo, T., Park, K. Y., Lee, Y. J., Ryu, S. E., Son, J. Y., Lee, J. U., and Heo, Y. S. (2016) Structural basis of checkpoint blockade by monoclonal antibodies in cancer immunotherapy. *Nat. Commun. 7*, 13354.

(27) Meuzelaar, H., Vreede, J., and Woutersen, S. (2016) Influence of Glu/Arg, Asp/Arg, and Glu/Lys Salt Bridges on e-Helical Stability and Folding Kinetics. *Biophys. J. 110*, 2328−2341.

(28) Daugherty, P. S., Chen, G., Iverson, B. L., and Georgiou, G. (2000) Quantitative analysis of the effect of the mutation frequency on the affinity maturation of single chain Fv antibodies. *Proc. Natl. Acad. Sci. U. S. A. 97*, 2029−2034.

DOI: 10.1021/acschembio.9b00743
ACS Chem. Biol. 2020, 15, 360−368

(29) Sidhu, S. S., Fairbrother, W. J., and Deshayes, K. (2003) Exploring Exploring Protein−Protein Interactions with Phage Display. *ChemBioChem 4*, 14−25.
(30) Flechner, E. R., Freudenthal, P. S., Kaplan, G., and Steinman, R. M. (1988) Antigen-specific T lymphocytes efficiently cluster with dendritic cells in the human primary mixed-leukocyte reaction. *Cell. Immunol. 111*, 183−195.
(31) Wing, K., Onishi, Y., Prieto-Martin, P., Yamaguchi, T., Miyara, M., Fehervari, Z., Nomura, T., and Sakaguchi, S. (2008) CTLA-4 control over Foxp3+ regulatory T cell function. *Science 322*, 271−275.
(32) Palucka, K., and Banchereau, J. (2013) Dendriticcell-based therapeutic cancer vaccines. *Immunity 39*, 38−48.
(33) Ha, D., Tanaka, A., Kibayashi, T., Tanemura, A., Sugiyama, D., Wing, J. B., Lim, E. L., Teng, K. W. W., Adeegbe, D., Newell, E. W., Katayama, I., Nishikawa, H., and Sakaguchi, S. (2019) Differential control of human Treg and effector T cells in tumor immunity by Fc-engineered anti-CTLA-4 antibody. *Proc. Natl. Acad. Sci. U. S. A. 116*, 609−618.
(34) Ingram, J. R., Blomberg, O. S., Rashidian, M., Ali, L., Garforth, S., Fedorov, E., Fedorov, A. A., Bonanno, J. B., Le Gall, C., Crowley, S., Espinosa, C., Biary, T., Keliher, E. J., Weissleder, R., Almo, S. C., Dougan, S. K., Ploegh, H. L., and Dougan, M. (2018) Anti-CTLA-4 therapy requires an Fc domain for efficacy. *Proc. Natl. Acad. Sci. U. S. A. 115*, 3912−3917.
(35) Chao, G., Lau, W. L., Hackel, B. J., Sazinsky, S. L., Lippow, S. M., and Wittrup, K. D. (2006) Isolating and engineering human antibodies using yeast surface display. *Nat. Protoc. 1*, 755−768.
(36) Tsudo, M., Uchiyama, T., and Uchino, H. (1984) Expression of Tac antigen on activated normal human B cells. *J. Exp. Med. 160*, 612−617.
(37) Julius, M. H., Simpson, E., and Herzenberg, L. A. (1973) A rapid method for the isolation of functional thymus-derived murine lymphocytes. *Eur. J. Immunol. 3*, 645−649.
(38) Kim, D. K., Fujiki, Y., Fukushima, T., Ema, H., Shibuya, A., and Nakauchi, H. (1999) Comparison of hematopoietic activities of human bone marrow and umbilical cord blood CD34 positive and negative cells. *Stem Cells 17*, 286−294.

DOI: 10.1021/acschembio.9b00743
ACS Chem. Biol. 2020, 15, 360−368